Effect of Coadsorbed Dopants on Diamond Initial Growth Processes: CH_3 Adsorption

T. Van Regemorter* and K. Larsson

Department of Materials Chemistry, Angstrom Laboratory, Uppsala University, Box 538, SE-751 21 Uppsala, Sweden

Received: December 3, 2007; Revised Manuscript Received: March 7, 2008

An investigation based on an ultrasoft pseudopotential density functional theory (DFT) method, using the generalized gradient approximation (GGA) under periodic boundary conditions, has been performed in order to investigate how the presence of a neighboring dopant is affecting the CH_3 adsorption reaction (regarded to be an initial growth process). For this study, both the (100) and (111) diamond surface orientations have been considered, and various dopants in two different hydrogenated forms AH_X (A = N, B, S, P, or C; X = 0 or 1 for S, X = 1 or 2 for N, B, and P, and X = 2 or 3 for C) were especially scrutinized. For most of the cases studied, the presence of a coadsorbed dopant was found to disfavor CH_3 adsorption with an efficiency that depends on the surface orientation as well as dopant type and position. The NH_2, PH_2, and SH species have the strongest effect in counteracting the CH_3 adsorption to the diamond (111) surface. This is also the situation with the dopants adsorbed on either of two specific surface sites (out of three positions studied) on the diamond (100)-2 × 1 surface. The main reasons for these observations are induced steric hindrances between the two coadsorbates. The BH_2 species, adsorbed to the third type of surface site on diamond (100), has been found to affect the adsorption reaction by formation of a C_{surf}−B bond prior to CH_3 adsorption. The dopants in their radical forms are generally shown to always strongly disfavor the CH_3 adsorption reaction by formation of a C_{surf}−X bond prior to adsorption. However, the NH radical will only form this new bond with the radical surface C site when it is adsorbed to position 3 on the surface.

I. Introduction

The surface chemistry involved in diamond growth using chemical vapor deposition (CVD) is very complex and implies competing gas-phase and surface reactions under the presence of various carbonaceous species. In an ordinary CVD setup, a small percentage (about 1−5%) of methane in a large excess of hydrogen (about 95−99%) is activated by specific methods (hot filament, plasma, laser, etc.). This gas-phase activation leads to a distribution of reactive carbonaceous species with a resulting concentration profile totally dependent on the activation type and different experimental variables (such as pressure, surface and gas temperature, gas flow, etc.).[1] For appropriate conditions, a certain sequence of surface reactions favoring diamond growth takes place. This sequence of reactions is generally divided into different reaction steps as adsorption, H abstraction, surface migration, etc.[2,3] The role played by the different gas-phase species and their importance for the growth mechanism are, however, still under debate.

It is a well-known fact that atomic hydrogen is sustaining the sp^3 hybridization of the surface carbon atoms in the diamond structure. Furthermore, gaseous hydrogen is known to take part in abstraction reactions during growth of diamond (leading to recombination products like H_2). The methyl radical (CH_3) is generally accepted as the main growth precursor, and the corresponding importance of CH_2 is still under debate.[4–7] The gas-phase composition in a microwave plasma-assisted CVD process was earlier theoretically studied in the work of Lombardi et al.[1] It was then found that the CH_3 density is more than 10 times larger than the CH_2 density in the gas phase next to the surface. This result is consistent with the early idea that this radical is the main precursor for diamond growth.[8,9] On the basis of these circumstances, only CH_3 has been assumed to be the adsorbed growth species in the present study.

Introduction of impurities (N, B, S, or P) into the diamond lattice is of major interest due to large effects on the properties of diamond (e.g., transformation to a semiconducting material). In choosing a suitable dopant for diamond one has to consider not only its effects on the diamonds properties but also its solubility and mode of incorporation.[10,11] It is possible to introduce the impurity during chemical vapor deposition (CVD) of diamond, and it has been observed experimentally that the presence of the dopant will largely affect the growth process (e.g., growth rate, surface smoothness, orientation).[12–15] In the presence of an impurity, important changes in the growth reaction steps have frequently been observed experimentally.[16–19] However, only a small number of theoretical publications have focused on this particular behavior, and many questions remain without answers.

The present paper shows some initial results regarding the influence of adsorbed dopants on an important elementary reaction occurring during diamond growth: adsorption of CH_3. The main question to be answered is if there is any dopant situation where CH_3 adsorption will be seriously counteracted or become extremely improved by the existence and type of a coadsorbed dopant. An induced hindrance of growth species adsorption would ultimately result in a transfer of this elementary reaction into a rate-limiting step (i.e., a bottleneck) for the whole diamond growth process. Careful density functional theory calculations under periodic boundary conditions have here been used in considering the N, P, S, and B (in two different hydrogenated forms) and their effect on the adsorption of CH_3 when coadsorbed to a neighboring surface site.

* To whom correspondence should be addressed.

10.1021/jp711402e CCC: $40.75
Published on Web 05/28/2008

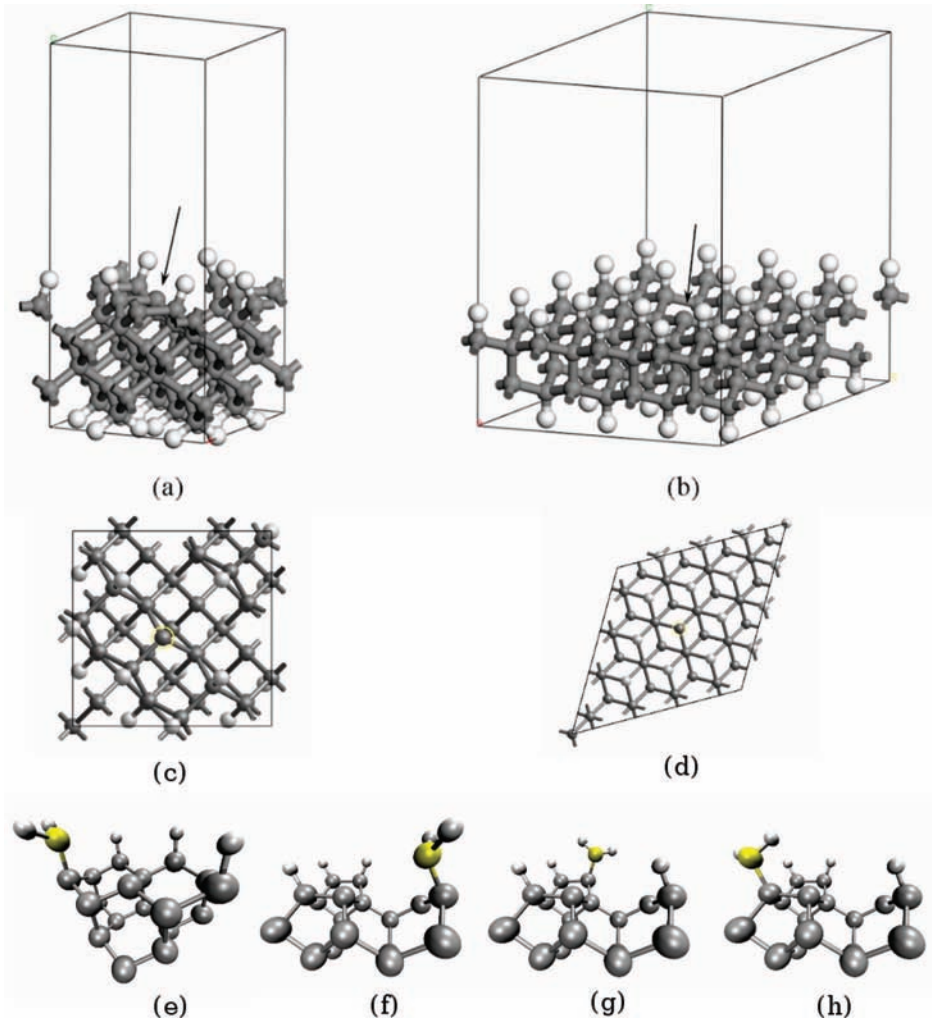

Figure 1. Representations of the supercells used in modeling the diamond (111) (a−c) and (100) (b−d) surfaces. The adsorption site for CH_3 is marked with an arrow in a and b. Various positions for coadsorption with a dopant (c) for the (111) surface and (d−f) for the three different possibilities on the (100) surface.

II. Methodologies

The present investigation was based on an ultrasoft pseudopotential density functional theory (DFT) method using the program package CASTEP from Accelrys, Inc.[20] The calculations were performed using the spin-polarized general gradient approximation and the PW91 functional (Perdew−Wang[21]) under periodic boundary conditions. Introduction of a density gradient is proven to give more accurate chemisorption energies compared to the spin-polarized local density approximation (LSDA).[22] However, the calculation time will unfortunately become dramatically increased for large model systems. In order to make the optimization procedure more practical, the geometry was first optimized using LSDA, followed by a single-point GGA-PW91 calculation on the final structure. The geometry optimizations were performed using the BFGS algorithm.[23] Careful test calculations were performed to ensure the reliability of this methodology. A comparison with direct geometry optimization using the GGA-PW91 functional resulted in a difference in total energy of less than 2% with no significant structural differences. The number of k points ($2 \times 2 \times 1$) was generated using the Monkhorst−Pack scheme,[24] and the cutoff energy was set to 280 eV. These values have been defined, after careful test calculations, to be the best compromise between the precision of the calculation and the calculation time. Indeed, higher values of these two parameters only showed an energy difference of about 1% in calculating the energy of adsorption for CH_3.

Both diamond (111) and (100) surfaces were included in the investigation, and the corresponding models are presented in Figure 1a−d, where the size of the supercell in the x and y directions determines the degree of adsorbate−surface coverage. These surfaces were H terminated, and the 2×1 reconstructed monohydride surface, (100)-2×1:H, was used in modeling the (100) surface. The optimal model parameters (i.e., number of C atomic layers, number of geometry-optimized layers, vacuum depth) were also determined by performing careful test calculations. It was shown that four and six carbon layers are enough to determine the CH_3 adsorption energy with a sufficient accuracy for the (111) and (100) surface, respectively. A further increase of the number of layers resulted in an increase in adsorption energy by less than 4% vs 1%. The greater number of layers required for convergence on the (100) surface is most probably the result from strains due to the surface dimer bonds. In addition, the most optimal numbers of relaxed atomic layers were found to be two and three for the (111) and (100) surface, respectively. A higher number of relaxed layers only resulted in CH_3 adsorption energy differences of smaller than 1%. For all test calculations, the lowest-lying carbon layers were frozen to simulate the constraint induced by the bulk. The periodic

reproduction of the unit cell along the z axis introduces a vacuum depth that must be large enough to avoid nonrealistic interslab interactions. From previous work, it is well known that 10 Å is an optimal value.[25] In conclusion, the diamond (100) surface is more sensitive with regard to both total number of C layers and number of relaxed C layers when studying the adsorption process of growth species.

For all calculations, the dopant species were adsorbed on a neighboring surface C site relative to the surface radical carbon onto which CH_3 will be adsorbed (the surfaces are presented in Figure 1a−d). Due to the high level of symmetry, all carbons surrounding a (111) adsorption site are equivalent (Figure 1e). Hence, the present study will be restricted to only one adsorption situation for the dopant/CH_3 combination on a diamond (111) surface. On the other hand, the much lower symmetry of the (100) surface has led to the consideration of three different positions for the dopant species relative to the CH_3 adsorption site (Figure 1f−h). In addition, the four most common diamond dopant elements have been considered in the study: N, P, B, and S. For each type of dopant, both fully hydrogenated and radical forms were considered (NH_2, NH, PH_2, PH, BH_2, BH, SH, and S). In order to outline the effect of these different dopants on the CH_3 adsorption, corresponding calculations on a fully hydrogenated surface and with a coadsorbed CH_3 were also performed. This comparative study will thereby make it possible to highlight the steric and electronic effects of the dopants on the initial growth reactions of diamond (111) and (100).

III. Results and Discussions

Effect of Dopants on the Adsorption of CH_3. ***A. General.*** Adsorption of a gaseous growth species onto the diamond surface is a very important elementary reaction in the CVD diamond growth process. It is also of greatest interest to define the energetic effect induced by the presence of a dopant bonded to a surface carbon neighboring the reactive adsorption site (i.e., the adsorption site for the growth species). The adsorption energy (ΔE_{ads}) has been calculated using

$$\Delta E_{ads} = E_{surface\text{-}ads} - (E_{surface} + E_{ads}) \quad (1)$$

where $E_{surface\text{-}ads}$ is the total energy for the finally adsorbed system and $E_{surface}$ (or E_{ads}) is the total energy for the nonadsorbed surface (or gaseous species). Since the atoms within the surface regions are allowed to be completely relaxed in the calculations, structural evolutions (before or after adsorption) may strongly affect the final numerical value of the adsorption energy. To be more specific, stabilization of the surface prior to adsorption will decrease the adsorption energy, while stabilization of the finally adsorbed system will improve it. The presence of an adsorbed dopant may cause this stabilization (or a corresponding destabilization) through interactions between itself and the reactive surface carbon site. The stabilization/destabilization may also occur through interactions between the adsorbed dopant and the adsorbed growth species (CH_3), and a combination of these effects is expected. In order to understand the numerical variation of the calculated CH_3 adsorption energies (as a function of types of dopant species), careful analysis of the geometrical and electronic structure of the system has to be performed.

B. CH_3 Adsorption Next to XH_2. The calculated energies for CH_3 adsorption to a (111) and a (100) diamond surface, with NH_2, PH_2, BH_2, or SH dopant species bonded to a neighboring surface carbon site, are presented in Table 1. These energies are compared with the adsorption energies obtained when the reaction occurs without any dopant on the surface (i.e., the adsorption site is only surrounded by hydrogen). In addition, the effects induced by the presence of a dopant are also compared with interactions generated by a neighboring CH_3 adsorbate. The purpose with this latter comparison is to highlight the effect of differences in electronegativity values between C and P, S, N, or B, which in turn may cause electronic delocalization effects within the surface region of the diamond lattice.

TABLE 1: CH_3 Adsorption Energies in the Presence of Different Adsorbed Dopants in Their Fully Hydrogenated Forms

		(100)		
ads E (kJ/mol)	(111)	pos 1	pos 2	pos 3
NH_2	−290.7	−317.9	−330.0	−349.6
PH_2	−266.0	−286.0	−298.9	−323.0
BH_2	−325.1	−366.2	−334.3	−268.5
SH	−270.6	−296.5	−305.6	−333.3
CH_3	−270.7	−289.6	−311.5	−329.7
H	−317.7		−358.5	

In Table 1, the energetic values show that the presence of NH_2, PH_2, or SH on a neighboring surface carbon will, for both diamond (111) and (100) surfaces, disfavor CH_3 adsorption. When compared to the situation with only H surface neighbors, the decrease in adsorption energy induced by a neighboring adsorbed NH_2 is relatively low [(111), 27 kJ/mol; (100), 8−40 kJ/mol]. In the presence of PH_2 or SH, the energetic reduction of the adsorption energy becomes more pronounced [(111), 52 vs 47 kJ/mol; (100), 35−72 vs 25−68 kJ/mol], which is comparable to the reduction obtained with a neighboring adsorbed CH_3 [(111), 47 kJ/mol; (100), 28−68 kJ/mol]. On the contrary, the presence of a neighboring BH_2 does not appreciably affect the CH_3 adsorption energy on the (111) surface (the adsorption energy is more pronounced by only 7 kJ/mol relative to the H scenario). Similarly, when the dopant is adsorbed in position 1 on the (100) surface, a slight improvement in the CH_3 adsorption energy is observed (of about 8 kJ/mol). On the other hand, the opposite is found for position 2, with a reduction in adsorption energy by 24 kJ/mol, and the decrease becomes drastically larger when attaching BH_2 in position 3 on (100) diamond (the difference drops as much as 90 kJ/mol).

For both of the (111) and (100) surfaces, the small reduction in adsorption energy observed when adsorbing CH_3 near an adsorbed NH_2 can be explained by steric repulsions. As a measure of the degree of CH_3−NH_2 repulsion, an angle α is defined by the surface plane (including the first carbon layer) and the $C_{surface}$−CH_3 bond in the plane formed by the two adsorbates (see Figure 2).

For each surface plane and each dopant position considered, Δα is defined as the difference between the α values for a NH_2 and an H neighbor. As can be seen in Figure 3, there is an obvious correlation obtained when relating Δα with the difference in corresponding adsorption energies.

The ΔE−Δα correlation gives a good argument for considering the steric repulsion between the coadsorbed CH_3 and NH_2

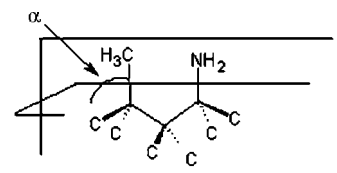

Figure 2. Definition of angle α.

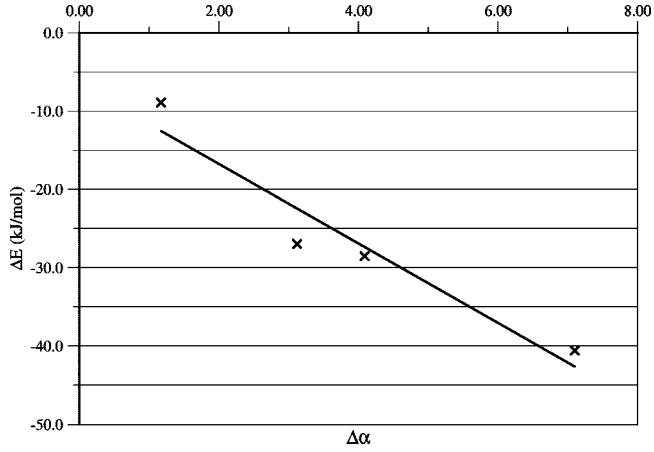

Figure 3. Graphical representation of the correlation between ΔE and $\Delta\alpha$. The individual data points are identified as $\Delta\alpha = 3.1$ for (111) and $\Delta\alpha = 7.1$ (position 1), 4.1 (position 2), and 1.2 (position 3) for (100).

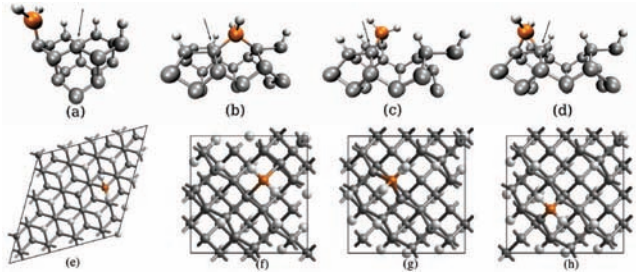

Figure 4. Optimized surface structure for an adsorbed BH_2 species next to the radical surface carbon (indicated by an arrow) prior to any CH_3 adsorption: (111) surface (a−c) and (100) surface with the dopant in position 1(b−f), 2 (c−g), and 3 (d−h), respectively.

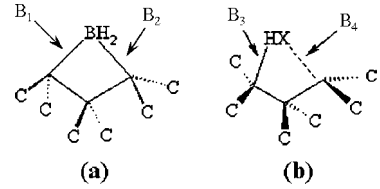

Figure 5. Definition of B_1, B_2, B_3, and B_4 as the distances between (a) BH_2 or (b) XH (X = N, P, S, or B) and the two neighboring surface carbons (prior to CH_3 adsorption).

TABLE 2: Values Observed for B_1 and B_2 on the (111) Surface and for the Three Different Positions on the (100) Surface when Using the BH_2 Dopant

		(100)		
	(111)	pos 1	pos 2	pos 3
B_1	no bond	1.81	1.72	1.60
B_2	1.56	1.81	1.72	1.60

species as the most important effect responsible for the small adsorption energy differences induced by the presence of an NH_2 dopant.

The negative effect on the CH_3 adsorption energy induced by neighboring PH_2 or SH adsorbate is also found to be due to steric repulsions between the adsorbed CH_3 and the respective dopant. Significant changes are observed for the angle α ($\Delta\alpha$ varies within the range of 4.1−7.4 for PH_2 and 2.8−7.0 for SH), but opposite to the situation with NH_2, it is not possible to find any direct correlation between $\Delta\alpha$ and ΔE. This is an indication that other effects are also responsible for the CH_3 adsorption energy variation.

In comparison to the effects induced by coadsorbate NH_2, PH_2, or SH (which are all affecting CH_3 adsorption by similar interactions), a neighboring BH_2 is affecting the CH_3 adsorption in a completely different way.

On both diamond (111) and (100), the resulting geometrical structure (after CH_3 adsorption) does not show any significant indication of steric repulsions between the coadsorbed BH_2 and CH_3. This can be explained by the fact that BH_2 has an empty p orbital with reduced steric hindrance, in contrast to NH_2, PH_2, and SH which have filled lone-pair orbitals. In comparison with the values obtained for a fully hydrogenated surface, the presence of BH_2 on the (111) surface is observed to change the CH_3 adsorption energy only 7 kJ/mol (Table 1). This similarity in adsorption energy is due to the lack of interconnections and geometrical constraints between the boron (in BH_2) and the surface C radical prior to CH_3 adsorption as can be seen in Figure 4a and 4e (and due to the absence of BH_2-CH_3 steric repulsions after the reaction, as mentioned earlier). However, for a neighboring adsorbed BH_2 species on the (100) diamond surface, the CH_3 adsorption energies (Table 1) appear to be much more influenced by the presence of BH_2. These energetic changes are induced by a $BH_2-C_{surface}$ interaction which occurs prior to CH_3 adsorption. This interaction is clearly visible for all three dopant positions in Figure 4b−d and 4f−h. From Table 1, the CH_3 adsorption appears to be most strongly affected by the presence of BH_2 in position 3 (a decrease of 90 kJ/mol relatively to the surface with only H neighbors). The corresponding differences for BH_2 in positions 1 and 2 are only a decrease of 24 kJ/mol for dopant site 2 and an increase of 8 kJ/mol for dopant site 1.

Prior to any CH_3 adsorption, analysis of the bond length formed between BH_2 and the two neighboring surface carbons (B_1 and B_2, as presented in Figure 5a) gives further information which helps in the understanding this unexpected behavior.

From Table 2, B_1 and B_2 bonds appear to be symmetric and become somewhat longer for BH_2 in position 1 or 2 (compared to position 3). These geometrical results indicate that the adsorption sites prior to methyl adsorption, for boron in position 1 and 2, are not as stabilized as in the situation with BH_2 in position 3. Moreover, the lengths of B_1 and B_2 for position 3 are very similar to the B_2 distance obtained for BH_2 adsorbed to the (111) diamond surface. This particular bond length (of 1.56 Å) can be considered as the "natural" $C_{diamond}-B$ bond length due to the low amount of constraints (adsorption of BH_2 to diamond (111) resulted in only one covalent bond). The decrease in CH_3 adsorption energy for position 3 on diamond (100) can thereby be explained by the more pronounced stabilization of the radical surface.

TABLE 3: CH_3 Adsorption Energies in the Presence of Different Dopants in Their Radical Form

			(100)	
ΔE_{ads} (kJ/mol)	(111)	pos 1	pos 2	pos 3
NH	−301.5	−355.3	−375.2	−229.1
PH	−218.3	−182.8	−195.7	−174.2
BH	−230.5	−196.6	−291.0	−127.8
S	−244.9	−243.1	−253.2	−221.9
CH_2	−274.3	−242.5	−244.3	−158.6
H	−317.7		−358.5	

The main goal with the present investigation has been to highlight the effects induced by a neighboring dopant on the CH_3 adsorption and compare these effects with the corresponding ones for only neighboring adsorbed H. However, the CH_3 adsorption next to a step is also important to consider for further carbon incorporation in the lattice. The effect of a dopant on this latter type of adsorption is therefore important to include in the present study. Two different growth steps exist on diamond (111), and theoretical studies have earlier shown that the CH_3 adsorption energies near step types A and B are, respectively, 14 and 142 kJ/mol (type A consists of (111) and (100) planes, while type B consists of only (111) planes).[26] The corresponding reaction energy obtained when adsorbing CH_3 next to an adsorbed CH_3, was calculated to be 199 kJ/mol.[27] Coadsorption next to a type B step, on diamond (111), may then be approached by studying CH_3 adsorption next to an already adsorbed CH_3. The difference in adsorption energies between the earlier and the present study can mainly be explained by the use of a cluster model, for the previous work, while an infinite surface slab is used for this investigation.

By extension, a step on both diamond (111) and (100) has been, rather coarsely, modeled using a CH_3 coadsorbates next to the adsorption site. By substituting C (from CH_3) with a dopant element (N, B, S, or P), a specific type of doped step is somehow modeled. Hence, a comparison of adsorption energies for CH_3 adsorbed near an already adsorbed CH_3 or an H-saturated dopant yields valuable information concerning the effect of dopants on CH_3 adsorption next to a growth step. With a neighboring NH_2 it is found that less steric hindrances are induced compared to a coadsorbed CH_3 species, resulting in slightly favored CH_3 growth species incorporation (i.e., adsorption): up to 40 kJ/mol. This effect might have some implications for the growth rate increase with N present in the CVD reactor (as observed experimentally).[13] The much larger sizes of PH_2 and SH (compared to NH_2) are observed to induce sterical repulsions numerically comparable in size with the ones induced by a coadsorbed CH_3 species. On the basis of these results, an effect on growth using these specific dopants is not expected. These observations are, however, in contradiction with experimental growth rate results which show clear effects by the presence of a dopant.[12,15] For BH_2 as coadsorbed dopant, the lack of steric repulsions with the adsorbed CH_3 results in adsorption energies that are numerically much more favored compared to values obtained with a coadsorbed CH_3 (instead of BH_2). Boron is thereby expected to favor carbon incorporation into the (111) surface. For the (100) surface, the coadsorbed BH_2 cannot be use to investigate the effect of boron in a step on the CH_3 adsorption due to the bond formation observed between BH_2 and the surface carbon radical prior to CH_3 adsorption.

C. Adsorption of CH_3 Next to XH. The calculated energies for adsorption of CH_3 to diamond (111) and (100) surfaces are presented in Table 3. Similar to the situation in section III.B, the dopants are positioned on a surface carbon neighboring the reactive adsorption site. The main difference is that the dopants are here in their radical form. The energetic values obtained in the presence of the radical dopants are then compared with the adsorption energies calculated without any dopant (i.e., by replacing the dopant with H). In addition, these values are also compared with the corresponding energies obtained with coadsorption of CH_2 on the neighboring surface carbon.

The adsorption energies presented in Table 3 show that, for both diamond (111) and (100) surfaces, the presence of a dopant in its radical form will almost always disfavor the CH_3 adsorption reaction. This is also the situation with the CH_2 coadsorbate. The exception is the NH* dopant, which will only disfavor CH_3 adsorption in position 3 on diamond (100). For the two other positions on diamond (100) and for the (111) surface, the presence of NH* does not affect CH_3 adsorption significantly.

For all cases investigated, the reduction of adsorption energy, induced by the presence of a dopant in its radical form, is due to formation of a new bond between the dopant and the reactive adsorption site (prior to CH_3 adsorption). The interaction between the radical surface carbon, C*, and the radical dopant is expected since these two surface radicals, when they are close to each others, tend to react and thereby reduce the surface energy (i.e., increase the stabilization) by forming a new bond (Figure 5b). In some cases, formation of this new bond induces too much constraint and only a weak interaction occurs. In order to study the intensity of this interaction, the distances between the dopant and the two neighboring surface carbons (B_3 and B_4) were compared (see Table 4).

As can be seen in Table 4 for the (111) surface and for positions 1 and 2 on the (100) surface, the large difference between B_3 and B_4 for the NH* dopant shows that two neighboring surface radicals (the adsorbed NH* and the surface C*) do not always manage to form a bond. The distance between the nitrogen (in NH*) and the reactive surface carbon is too long to create a B_4 bond without causing severe geometrical constraints. This lack of strong C*−NH* interaction is here correlated to the small energetic difference in CH_3 adsorption energy for the various dopant position sites (16 kJ/mol for (111), 3 kJ/mol for position 1 on (100), and 17 kJ/mol for position 2 on (100)). The situation is however different for NH* in position 3 on the (100) surface. The C*−NH* distance is much shorter, and B_4 bond formation explains the large decrease in the CH_3 adsorption energy of about 129 kJ/mol (see Table 3).

With PH* adsorbed on the neighboring carbon site, the identical values obtained for B_3 and B_4 indicate that a second bond is always formed between the radical PH* adsorbate and the reactive surface carbon site (C*). This is the situation for both the (111) surface as well as for the different positions (1, 2, and 3) on the (100) surface. Compared to the NH* dopant, the tendency to form stable bonds can be explained by the fact that C*−-PH* is a longer and more flexible bond due to occupation of the more diffuse 3s and 3p orbitals on P. Formation of this new C*−PH* bond will thereby strongly affect the adsorption of CH_3. In relation to the situation with only neighboring H adsorbates on the surface, the CH_3 adsorption energy decreases by about 99 kJ/mol for the diamond (111) surface and 176, 163, and 184 kJ/mol for positions 1, 2, and 3 on the diamond (100) surface when introducing a neighboring PH* dopant on the surface.

The bond distances (B_3 and B_4) presented in Table 4 for the diamond (100) surface show that adsorbed radical sulfur (S*) has a similar effect as PH*. For all three different positions

TABLE 4: Values of the Distances B_3 and B_4 (Å) between the Adsorbed Dopant and the Two Binding Surface Carbon Atoms

	NH*				PH*				S*			
		(100)				(100)				(100)		
	(111)	pos 1	pos 2	pos 3	(111)	pos 1	pos 2	pos 3	(111)	pos1	pos 2	pos 3
B_3	1.42	1.41	1.40	1.46	1.99	1.99	1.92	1.83	1.82	1.98	1.90	1.79
B_4	2.74	2.66	2.75	1.46	1.99	1.99	1.92	1.83	2.81	1.98	1.90	1.79

	BH*				CH_2*			
		(100)				(100)		
	(111)	pos 1	pos 2	pos 3	(111)	pos 1	pos 2	pos 3
B_3	1.63	1.68	1.57	1.51	1.66	1.63	1.61	1.50
B_4	1.63	1.68	1.57	1.51	1.66	1.63	1.61	1.50

considered, formation of a new bond between S* and the surface radical (C*) is observed. The CH_3 adsorption energy is hence also strongly affected by a reduction of 115 (position 1), 105 (position 2), and 137 (position 3) kJ/mol, respectively. On the other hand, the large difference between the bond lengths B_3 and B_4 on the (111) surface indicates that there is no bond formation between S* and C*. However, there must be some type of electronic interactions between these two radicals since the S* dopant causes, also for this surface, an important decrease in CH_3 adsorption energy (by about 73 kJ/mol).

For the situation with an adsorbed radical BH*, a strong decrease in CH_3 adsorption energy (in the range 68−231 kJ/mol) is observed. The values presented in Table 3 show that the CH_3 adsorption energy has the largest decrease when the neighboring BH* species is adsorbed in position 3 on diamond (100) (231 kJ/mol). When the dopant is in position 1, the effect induced by the neighboring BH* species decreases (the energetic difference becomes 162 kJ/mol). The decrease becomes even smaller (about 128 kJ/mol) for the (111) diamond surface, and finally, the smallest energetic reduction (of about 68 kJ/mol) is reached when BH* is in position 2 on diamond (100). The observed difference in adsorption energy for the four surface situations can again be explained by performing a careful analysis of the surface structure before and after CH_3 adsorption. Prior to the adsorption reaction, the large similarity between B_3 and B_4 (Table 4) indicates that a new C*−BH* bond is created. Here again, the smallest C*−BH* bond length observed for position 3 on the (100) surface is responsible for the largest change observed in the CH_3 adsorption energy.

Structural analysis of the surface after CH_3 adsorption generally did not show any significant interaction between the dopant and the adsorbed CH_3 species. The only exception is the specific rearrangement which was observed for the (111) diamond surface and for the (100) diamond surface with the BH* dopant in position 2. Analysis of the surface structure after CH_3 adsorption shows that an H atom is transferred from the adsorbed CH_3 to the neighboring BH* species. Two new coadsorbed species (CH_2 and BH_2) are present, and a new C−B bond is thereby formed by an overlap of the empty p orbital from the boron and the orbital containing the unpaired electron within CH_2. The negative effect induced by C*−BH* bond formation prior to CH_3 adsorption is thereby counteracted by this stabilization, resulting in an adsorption reaction that is less energetically disfavored (Table 3).

A comparison of the effects induced by a coadsorbed radical dopant and a radical CH_2 species gives the possibility of highlighting specific interactions which are characteristic for the dopant. It is observed that PH*, S*, and BH* are affecting the CH_3 adsorption somewhat similarly to a coadsorbed CH_2 species. For both types of coadsorbed species, the reaction is disfavored due to formation of a new bond between the surface radical carbon (prior to CH_3 adsorption) and the radical dopant (or CH_2 species). The presence of a coadsorbed radical dopant is then expected to not disfavor more the diamond CVD growth than a coadsorbed CH_2 would. On the other hand, NH* is expected to have a small positive effect on the growth since no new N−C bond is formed prior to CH_3 adsorption, which might slightly increase the amount of free surface carbon radical.

IV. Conclusion

The purpose of this study was to carefully analyze the effect of four different types of coadsorbed dopants (N, P, S, and B), in both their fully hydrogenated and radical forms, on CH_3 adsorption onto two different diamond surface planes: (111) and (100). The calculations were performed under periodic boundary conditions using DFT methods based on a spin-polarized GGA-PW91 functional and a plane-wave basis set.

The CH_3 adsorption reaction was found to be mainly affected by steric repulsions when coadsorbed with a neighboring dopant such as NH_2, PH_2, or SH. The degree of steric hindrance was then correlated to the size of the dopant. However, minor electronic interactions are expected to also affect CH_3 adsorption in coadsorption with PH_2 or SH. For the (111) surface, the presence of BH_2 was not found to affect the CH_3 adsorption energy either by (i) an interaction with the surface C* site prior to adsorption or (ii) an interaction with the finally adsorbed CH_3 species. For the (100) surface, the presence of BH_2 was not found to interact with the finally adsorbed CH_3 species. However, an unexpected interaction with the radical surface carbon, C*, was found to occur prior to CH_3 adsorption. With BH_2 coadsorbed in position 3, the neighboring CH_3 adsorption was found to be largely disfavored due to formation of a strong C*−BH_2 bond. However, this type of C*−BH_2 interaction was not found to be that significant and hence not affecting the CH_3 adsorption to any appreciably extent with BH_2 in position 1 or 2.

Coadsorbed dopant radicals (NH*, PH*, S* and BH*) were, with few exceptions, found to always disfavor the CH_3 adsorption reaction due to formation of a stabilizing new bond between the dopant and the surface radical carbon, C*, prior to CH_3 adsorption. The PH* dopant adsorbate was found to be most efficient in lowering the CH_3 adsorption energy, and this effect is, compared to the effect on diamond (111), also twice as strong for all three dopant positions on the (100) surface. For the S* dopant, the variation in CH_3 adsorption energy was found to be generally much smaller compared to the values obtained in the presence of PH* on the surface. For both PH* and SH* coadsorbates on diamond (111), CH_3 adsorption became energetically more disfavored compared to the situation when there

is instead a neighboring CH_2* adsorbate. For the (100) surface and dopant positions 1 and 2, the energetic variations using CH_2* were rather similar to the values obtained for SH*. However, when CH_2* was in position 3, CH_3 adsorption became much more negatively affected and the energetic difference became similar to the value obtained with PH* as a neighboring adsorbate.

The presence of NH* on the surfaces resulted in a specific behavior. This dopant was not found to predominantly affect the CH_3 adsorption reaction on the (111) surface or on the (100) surface in position 1 and 2. However, when adsorbed in position 3 on the (100) surface, CH_3 adsorption became strongly disfavored due to a bond formation between NH* and the surface radical C* prior to CH_3 adsorption. The presence BH* on the surface showed the most intriguing effect on the CH_3 adsorption. For the (100) surface and with BH* in position 1 or 3, CH_3 adsorption was only affected (as for the other dopants PH*, S*, or CH_2*) by C−X (X = P, S, or C) bond formation. For the two other situations (for the (111) surface and for BH* in position 2 on the (100) surface), the BH* adsorbate showed a particular capability to capture an H atom from the coadsorbate CH_3 followed by formation of a new bond between the resulting coadsorbed CH_2* and BH_2 species. The stability of the final surface structure was thereby increased and CH_3 adsorption less disfavored. It is important to keep in mind that even if the reaction is less disfavored due to this extra stabilizing effect induced by the final surface structure, the reaction is expected to be still strongly affected by C*−BH* bond formation prior to adsorption.

Acknowledgment. This work was supported by the European Project RTN DRIVE from the 6th Framework Programme (no. MRTN-CT-2004-512224).

References and Notes

(1) Lombardi, G.; Hassouni, K.; Stancu, G.; Mechold, L.; Röpcke, J.; Gicquel, A. *J. Appl. Phys.* **2005**, *98*, 053303.
(2) Larsson, K.; Carlsson, J. *Phys. Rev.* **1999**, *59*, 8315–8322.
(3) Netto, A.; Frenklach, M. *Diamond Relat.* **2005**, *14*, 1630–1646.
(4) Battaile, C. C.; Srolovitz, D. J.; Butler, J. E. *J. Appl. Phys.* **1997**, *82*, 6293–6300.
(5) D'Evelin, M. P.; Graham, J. D.; Martin, L. R. *Diamond Relat.* **2001**, *10*, 1627–1632.
(6) Larsson, K.; Lunell, S.; Carlsson, J. *Phys. Rev. B* **1993**, *48*, 2666–2674.
(7) Battaile, C. C.; Srolovitz, D.; Oleinik, I.; Pettifor, D. G.; Sutton, A. P. *J. Chem. Phys.* **1999**, *111*, 4291–4299.
(8) Martin, L. R.; Michael, W. H. *Appl. Phys. Lett.* **1989**, *55*, 2248–2249.
(9) Harris, S. J. *Appl. Phys. Lett.* **1990**, *56*, 2298–2300.
(10) Larsson, K. *Comp. Mater. Sci.* **2003**, *27*, 23–29.
(11) Kajihara, S. A.; Antonelli, A.; Bernholc, J. *Physica B* **1993**, *185*, 144–149.
(12) Haubner, R. *Diamond Relat. Mater.* **2005**, *14*, 355–363.
(13) Silva, F.; Gicquel, A. *Electrochem. Soc. Proc.* **1997**, *97−32*, 99–125.
(14) Locher, R.; Wild, C.; Herres, N.; Behr, D.; Koidl, P. *Appl. Phys. Lett.* **1994**, *65*, 34–36.
(15) Sternschulte, H.; Schreck, M.; Stritzker, B.; Bergmaier, A.; Dollinger, G. *Diamond Relat. Mater.* **2003**, *12*, 318–323.
(16) Frauenheim, Th.; Jungnickel, G.; Sitch, P.; Kaukonen, M.; Weich, F.; Wildany, J.; Poreza, D. *Diamond Relat. Mater.* **1998**, *7*, 348–355.
(17) Zhou, H.; Yokoi, Y.; Tamura, H.; Takami, S.; Kubo, M.; Miyamoto, A.; Gamo, M. N.; Ando, T. *Jpn. J. Appl. Phys.* **2001**, *40*, 2830–2832.
(18) Tamura, H.; Zhou, H.; Takami, S.; Kubo, M.; Miyamoto, A.; Gamo, M. N.; Ando, T. *J. Chem. Phys.* **2001**, *115*, 5284–5291.
(19) Cheesman, A.; Harvey, J. N.; Ashfold, M. N. R. *Phys. Chem. Chem. Phys.* **2005**, *7*, 1121–1126.
(20) Segall, M. D.; Shah, R.; Pickard, C. J.; Payne, M. C. *J. Phys.: Condens. Matter* **2002**, *14*, 2717–2743.
(21) Perdew, J. P. *Physica B* **1991**, *172*, 1–6.
(22) Perdew, J. P.; Chevary, J. A.; Vosko, S. H.; Jackson, K. A.; Pederson, M. R.; Singh, D. J.; Fiolhais, C. *Phys. Rev. B* **1992**, *46*, 6671–6687.
(23) Pfrommer, B. G.; Côté, M.; Louie, S. G.; Cohen, M. L. *J. Comput. Phys.* **1997**, *131*, 233–240.
(24) Monkhorst, H. J.; Pack, J. D. *Phys. Rev. B* **1976**, *13*, 5188–5192.
(25) Petrini, D.; Larsson, K. *J. Phys. Chem. B* **2005**, *109*, 22426–22431.
(26) Larsson, K. *Phys. Rev. B* **1997**, *56*, 15452–15458.
(27) Larsson, K.; Carlsson, J.-O.; Lunell, S. *Phys. Rev. B* **1995**, *51*, 10003–10012.

JP711402E